

Cementum and enamel surface mimicry influences soft tissue cell behavior

Benjamin Bellon^{1,2,3} | Benjamin Pippenger^{2,4} | Alexandra Stähli⁴ | Martin Degen⁵ | Ludovica Parisi⁵

¹Faculty of Medicine and Health Technology, University of Tampere, Tampere, Finland

²Preclinical and Translational Research, Institut Straumann AG, Basel, Switzerland

³Clinic of Conservative and Preventive Dentistry, University of Zurich, Zürich, Switzerland

⁴Department of Periodontology, University of Bern, Bern, Switzerland

⁵Laboratory for Oral Molecular Biology, Department of Orthodontics and Dentofacial Orthopedics, University of Bern, Bern, Switzerland

Correspondence

Ludovica Parisi, Laboratory for Oral Molecular Biology, Department of Orthodontics and Dentofacial Orthopedics, University of Bern, Bern, Switzerland.

Email: ludovica.paris@unibe.ch

Abstract

Aims: To test whether titanium surface roughness disparity might be used to specifically guide the behavior of gingiva fibroblasts and keratinocytes, thereby improving the quality of soft tissue (ST) integration around abutments.

Methods: Titanium discs resembling the roughness of enamel (M) or cementum (MA) were created with normal or increased hydrophilicity and used as substrates for human fibroblasts and keratinocytes. Adhesion and proliferation assays were performed to assess cell-type specific responses upon encountering the different surfaces. Additionally, immunofluorescence and qPCR analyses were performed to study more in depth the behavior of fibroblasts and keratinocytes on MA and M surfaces, respectively.

Results: While enamel-like M surfaces supported adhesion, growth and a normal differentiation potential of keratinocytes, cementum-emulating MA surfaces specifically impaired the growth of keratinocytes. Vice versa, MA surfaces sustained regular adhesion and proliferation of fibroblasts. Yet, a more intimate adhesion between fibroblasts and titanium was achieved by an increased hydrophilicity of MA surfaces, which was associated with an increased expression of elastin.

Conclusion: The optimal titanium implant abutment might be achieved by a bimodal roughness design, mimicking the roughness of enamel (M) and cementum with increased hydrophilicity (hMA), respectively. These surfaces can selectively elicit cell responses favoring proper ST barrier by impairing epithelial downgrowth and promoting firm adhesion of fibroblasts.

KEYWORDS

dental abutments, fibroblasts, hydrophilicity, keratinocytes, roughness, soft tissue integration

Martin Degen and Ludovica Parisi authors gave equal contribution to the manuscript.

This is an open access article under the terms of the [Creative Commons Attribution-NonCommercial-NoDerivs](https://creativecommons.org/licenses/by-nc-nd/4.0/) License, which permits use and distribution in any medium, provided the original work is properly cited, the use is non-commercial and no modifications or adaptations are made.

© 2024 The Author(s). *Journal of Periodontal Research* published by John Wiley & Sons Ltd.

1 | INTRODUCTION

Long-term survival of titanium dental implants is mainly determined by the intimate structural and functional connection that is created at the interface with the surrounding bone (i.e., osseointegration).¹ However, to ensure a successful clinical outcome, the establishment of an effective and tight soft tissue (ST) barrier around the transmucosal component seems as important as osseointegration.² Indeed, the formation of a proper biological seal is crucial to protect the bone-to-implant interface from pathogenic microorganisms present in the oral cavity, which can cause inflammatory reactions progressing into severe damages of the peri-implant tissues and leading, in the most severe cases, to implant failure.³ Furthermore, proper ST organization around abutments is also important, especially in the esthetic zone, as the appearance of the tissues should reflect those of the adjacent natural teeth.⁴

Advances and innovations in the healthcare field have usually evolved by recapitulating the solutions provided by nature, a practice often referred to as "biomimicry".⁵ Yet, there are some biological structures that cannot be copied from healthy periodontal to peri-implant ST. These include the periodontal ligament (PDL) as well as the junctional epithelium (JE).^{6,7} Because of the lack of the PDL, the implant cannot be firmly attached to the neighboring alveolar bone by perpendicular Sharpey's fibers. Rather, it is surrounded by collagen fibers, which are synthesized, and assembled by gingival fibroblasts, and which run parallel to the inert titanium surface.⁸⁻¹⁰ This results in poorer mechanical resistance of the transmucosal component when compared with the situation around natural teeth. In addition, the most apical epithelium that is formed around dental implants is different to the JE adjacent to teeth as it is not derived from the reduced enamel epithelium and hence, cannot encapsulate all the unique properties of the JE.^{6,11,12} Furthermore, the newly formed epithelial seam around dental implants is shorter and more apically attached when compared to the native situation, creating a deeper pocket more vulnerable for bacterial infections.^{2,8} Collectively, the situation around abutments is not identical to the natural system, which might contribute to the challenges related to the formation of a proper biological seal (i.e., reduced stability, bacterial accumulation).

Although we cannot entirely reproduce the physiological ST organization around teeth, we still aim to biomimic as much as possible from it with the hope to further boost the clinical success of implants. Specifically, we focused on titanium surface roughness and wettability as key parameters known to affect cell responses.¹³⁻¹⁵ It has been shown that microrough surfaces promote osteoblast differentiation and osteogenesis,^{16,17} as well as macrophage polarization into a pro-reparative M2 phenotype.¹⁸ Similar, hydrophilicity of such surfaces can further promote these cellular processes enhancing the overall performance of dental implants.¹⁹⁻²² Yet, the impact of titanium surface roughness and hydrophilicity on ST cells (i.e., fibroblasts and keratinocytes) is still a relatively unexplored research topic.

As enamel and cementum interfacing the JE keratinocytes and PDL fibroblasts, respectively, display inherently different

roughness,²³ we hypothesized that this roughness disparity might elicit cell type specific responses relevant for ST barrier formation around abutments. Titanium implants mimicking the surface roughness of natural enamel and cementum were created that allowed us to assess surface-mediated behavior of gingiva keratinocyte and fibroblasts, the most relevant cell types in contact with the abutment. Through a series of in vitro assays, we could show that bimodal titanium surface roughness can potentially guide the response of ST cells, which might maximize the success of clinical implants by providing a better ST integration around the abutment.

2 | MATERIALS AND METHODS

2.1 | Histology

Six Göttingen Minipig (Ellegaard Göttingen Minipigs) unextracted molars and premolar, which were obtained as discarded material, were used to clarify the anatomy of ST adhesion around tooth neck. To do that, teeth were processed for hard tissue histology as previously described²⁴ and stained with hematoxylin-eosin (H&E).

2.2 | Minipig teeth collection and preparation for surface roughness analysis

Similarly, in order to analyze the surface roughness of natural teeth and to generate biomimetic surfaces, 18 Göttingen Minipig teeth (12 premolars and 6 molars) were collected as discarded material from other approved studies and placed into 70% ethanol. Before the analysis of surface roughness, teeth were removed from ethanol, air dried and placed into a sputter coater (208 HR, Cressington Scientific Instrument) to be coated with a 7 nm layer of Platinum/Palladium to reduce reflective artifacts in the roughness measurement process.

2.3 | Titanium discs

Titanium discs with a machined (M) or a treated (MA) surface were developed, manufactured, and provided by Institute Straumann AG as follows. The SLA surface method was adapted specifically by removing the sandblasting step and adjusting the acid treatment process until the desired surface roughness was obtained. Half of the M and MA surfaces were further treated, following the same manufacturing process of the SLActive surface generation (wet chemical method) to increase their hydrophilicity, obtaining hM and hMA surfaces, respectively. Increase of surface hydrophilicity was confirmed through water contact angle measurements using a sessile-drop test with ultrapure water (EasyDrop DSA20E, Krüss GmbH).

Samples were provided as sterile discs of 1 mm (thickness) and 15 mm (diameter) to fit in 24-well culturing plates.

2.4 | Surface roughness analysis

Tooth and titanium disc surface roughness were measured with a confocal microscope (S neox 090 non-contact 3D Optical Profilometer, Sensofar AG). Three titanium discs for each group were assessed at three random positions. For each of the 18 evaluated teeth, the area of interest corresponding to the enamel and the cementum was manually selected in the proximity of the cemento-enamel junction (CEJ) which showed as a clearly visible margin. Measurements of the cementum were taken from the coronal most portion. 3D images were obtained with the confocal microscope equipped with a 20X lens on a measurement area of $842 \times 707 \mu\text{m}^2$ with a lateral resolution of $0.69 \mu\text{m}$. The 3D roughness parameters were calculated with the software SensoMAP Premium (Sensofar AG) by applying a Gaussian filter with a cutoff wavelength of $30 \times 30 \mu\text{m}^2$.

2.5 | Cell culture

Patient-matched primary human gingiva-derived keratinocytes (hGK) and fibroblasts (hGF) were isolated and purified using the explant culture technique from discarded biopsies obtained from the retromolar area of patients undergoing dental treatments in the Department of Periodontology, University of Bern, Switzerland.²⁵ Primary gingiva keratinocytes as well as the immortalized oral mucosa keratinocyte line OKF6/TERT-2 were grown in keratinocyte serum-free medium (KSFM, Thermo Fisher Scientific) containing $25 \mu\text{g/mL}$ bovine pituitary extract, 0.2 ng/mL epidermal growth factor, 0.4 mM CaCl_2 , and 1% penicillin and streptomycin (PenStrep, Thermo Fisher Scientific), while fibroblasts were cultured in Dulbecco's Modified Eagle's Medium with 10% fetal bovine serum (FBS, Sigma-Aldrich) and 1% PenStrep as described elsewhere.^{25,26} For all the experiments using single cell types, keratinocytes and fibroblasts were seeded on titanium discs at an initial concentration of 10000 cells/disc (adhesion assay) or 1000 cells/disc (viability and differentiation assay); while for co-culture experiments, hGK and hGF were seeded in a 1:1 ratio with 5000 keratinocytes and 5000 fibroblasts/disc and cultured for 5 days in a 1:1 medium as previously reported.²⁷ Details about cells used in this study are reported in Table 1. Culturing media were exchanged every other day.

TABLE 1 List of the cells used.

ID	Cells	Donor sex	Donor age (years)	Origin
hGK	Keratinocytes	F	28	Retromolar pad
hGF	Fibroblasts			gingiva primary
OKF6/TERT-2	Keratinocytes	M	57	Floor of the mouth immortalized

2.6 | Immunofluorescence staining

For Immunofluorescence (IF) staining, cells were washed twice with phosphate-buffered saline (PBS) before fixation in 4% paraformaldehyde (PFA) for 20 min at room temperature (RT). Cells were then washed 3X with PBS, permeabilized in 0.1% Triton-X-100 for 5 min, and rinsed three times with PBS prior to blocking in 3% bovine serum albumin solution for 30 min at RT, followed by incubation with primary antibody for 2 h at RT. Afterward, cells were extensively rinsed in PBS and incubated with fluorescent-labelled secondary goat anti-mouse/rabbit antibodies (dilution 1:1000; Molecular Probes, Thermo Fisher Scientific) with or without tetramethylrhodamine (TRITC)-phalloidin (dilution 1:50; Sigma-Aldrich) for 1 h at RT in the dark. Finally, cells were washed 3X in PBS and once with double-distilled water (ddH_2O) before being coverslip-mounted using the Vectashield Mounting Medium containing DAPI (Vector Laboratories). Samples were examined under an Olympus BX51 phase/fluorescence microscope (Olympus Life Science Solutions) equipped with fluorescence filters U-MWIBA3 for Alexa Fluor 488, U-MWIGA3 for Alexa Fluor 568, and U-MNUA2 for DAPI (Olympus Life Science Solutions) detection.

Primary antibodies used: Mouse monoclonal antibodies anti-vinculin (dilution 1:100; V9131, Sigma-Aldrich), anti-laminin $\alpha 3$ (dilution 1:100; P3H9, Developmental Studies Hybridoma Bank), anti-keratin 10 (dilution 1:100; DE-K10, Thermo Fisher Scientific), and anti-involucrin (dilution 1:100; SY5, BIO-RAD). Rabbit polyclonal antibodies anti-fibronectin,²⁸ anti-keratin 13 (dilution 1:100; Proteintech), and anti-transglutaminase 1 (dilution 1:200; Thermo Fisher Scientific).

2.7 | Cell adhesion

hGK, hGF and OKF6/TERT-2 cells were seeded on M and MA titanium discs at a density of 10000 cells/disc in their respective culture medium. After 3 h, 24 h, and 7 days, cells were gently washed with PBS and fixed in 4% PFA for 20 min at RT. After extensive washing with PBS and ddH_2O , cells were coverslip mounted with the Vectashield Mounting Medium containing DAPI (Vector Laboratories). Samples were examined under an Olympus BX51 phase/fluorescence microscope (Olympus Life Science Solutions). Images were analyzed using the ImageJ software.

2.8 | Cell viability

To evaluate the number of viable hGF and OKF6/TERT-2 cells on M and MA titanium implant surfaces, an MTT (3-(4,5-dimethylthiazol-2-yl)-2,5-diphenyltetrazolium bromide) assay was performed 2, 4, and 6 days after seeding 1000 cells/disc in their complete culturing medium. At each experimental time point, cells were incubated with MTT solution (Sigma-Aldrich) at a final concentration of 0.5 mg/mL for 4 h to allow MTT conversion into formazan in metabolically active cells. After two PBS washes, converted MTT was solubilized with a 4 N HCl solution, and the absorbance read at 570 nm on an EL808 BioTek microplate reader (BioTek).

2.9 | In vitro differentiation of keratinocytes

To induce keratinocyte differentiation, a cell density-dependent assay was applied. In brief, keratinocytes were grown in complete KSFM, plated on M or hM titanium discs at a density of 1000 cells/disc density, and grown for 7 days to reach full confluence before harvesting. In parallel, cells were also seeded on plastic (1000 cells/well of a 24-well plate) and collected after 2 days of culture, as the emergence of the first colonies was observed. Cells grown on plastic were used as the normalizing low-density (LD) sample.

Alternatively, for cell characterization, hGK and OKF6/TERT-2 cells were cultured in basal KSFM medium (0.1 mM CaCl_2) to bring them to a basal differentiation state. After 3 days in basal medium, 100 000 cells were seeded into 60 mm tissue culture dishes in basal medium. Twenty-four hours later, CaCl_2 was adjusted to a final 1.8 mM concentration (Calcium switch) and incubated for another 3 days to induce differentiation.

2.10 | RNA extraction, cDNA synthesis, and quantitative real-time polymerase chain reaction (qPCR)

At the end of the culturing time, total RNA from living cells was extracted using the innuPREP RNA Mini Kit (IST Innuscreen GmbH) following the manufacturer's instructions. RNA concentration was measured with a NanoDrop 2000c (Thermo Fisher Scientific) and stored at -80°C until use.

cDNA was synthesized starting from 500 ng of total RNA using an Oligo(dT)₁₅ primer (Microsynth AG) and the M-MLV reverse transcriptase (Promega).

Gene expression was analyzed in triplicate by qPCR using the GoTaq® qPCR Master Mix (Promega) on a QuantStudio 3 instrument (Applied Biosystems, Thermo Fisher Scientific) using a 10 μL reaction, with the following cycling program: 40 cycles of 15 s at 95°C followed by 1 min at 60°C were applied.

Data analysis was performed using the ΔC_T method when absolute mRNA normalized to *GAPDH* levels were reported or by $\Delta\Delta\text{C}_T$

method when absolute levels were further referenced to a control sample.

The sequences of the qPCR primers used are listed in Table S1. Primers were taken from the NCBI primer designing tool and tested for specificity and efficiency using cDNA standard curves.

2.11 | Statistical analysis

Experiments were performed at least three times in multiple replicates. Data were analyzed using Prism 7 (GraphPad) and reported as means \pm standard deviation (SD). Comparisons between two groups were performed using the Mann-Whitney nonparametric test. Multiple comparisons were performed using one- or two-way analysis of variance (ANOVA) with Tukey's post hoc test, after having assessed the normality of the data using the Shapiro-Wilk normalization test. Data were considered significant when $p < .05$.

3 | RESULTS

3.1 | Bimodal roughness can be used to mimic the interface between periodontal soft tissues and tooth

We initially inspected the naturally occurring interactions of the periodontal ST with the tooth structures. H&E staining of porcine teeth illustrated that the JE keratinocytes attached to the enamel, while the connective tissue (CT) cells (i.e., PDL fibroblasts) were associated to the cementum, with the CEJ representing a sharp border separating the two tissue compartments (Figure 1A). Prompted by this observation, we were keen to learn whether the surface roughness disparity between enamel and cementum is responsible for this strict cell type discrimination. Aiming to emulate the physiological surface modalities, we initially measured the surface roughness of enamel and cementum of porcine teeth. We observed a stark shift from a smooth (enamel) to a rougher surface (cementum) around the level of the CEJ (Figure 1B). These measurements allowed us to create machined (M) and surface treated titanium discs (MA) with Sa values similar to the ones of natural enamel and cementum, respectively (Figure 1C). Notably, the ratio of the physiological cementum/enamel surface roughness could be optimally recapitulated with the newly generated titanium discs (MA/M) (Figure 1D). Verification of the various surfaces resulted in hydrophobic and hydrophilic surfaces consistent with values typical to SLA and SLActive, respectively.²⁹

These observations provided the rationale for using the novel titanium discs to test whether the surface roughness disparity might be used to specifically guide attachment and growth of hGF and hGK to improve the quality of the peri-implant ST.

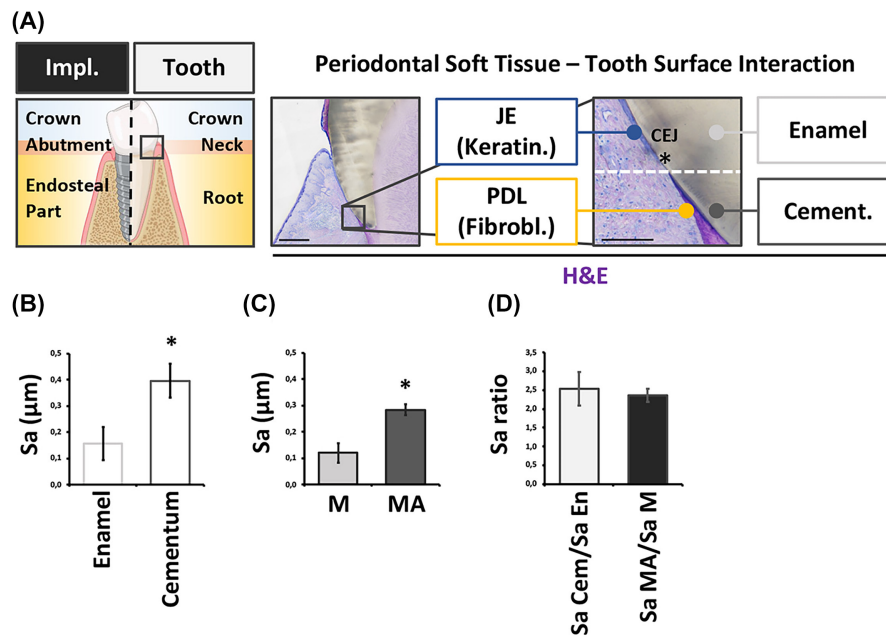


FIGURE 1 Fabrication of titanium discs mimicking the tooth surface roughness at the interface with periodontal soft tissues. (A) Diagram depicting the interaction of periodontal and peri-implant tissues with tooth and implant components, respectively. Hematoxylin and Eosin (H&E) staining of embedded porcine teeth at the level of the cementum-enamel junction (CEJ) highlights that the keratinocytes constituting the junctional epithelium (JE) are in direct contact with the enamel, while the fibroblasts of the soft connective tissue (PDL) interface the cementum. Scale bar: 500 μm . Close-up (right image): 250 μm . (B) Histogram reporting average roughness values of enamel and cementum. Based on such values titanium discs were produced with similar roughness values. * $p < .05$. (C) Corresponding histogram showing roughness of newly produced enamel-like (M) and cementum-like (MA) surfaces. * $p < .05$. (D) Histogram depicting the ratio between the roughness of cementum and enamel, and of M and MA surface.

3.2 | In competing systems, titanium model substrates emulating the roughness of cementum favor gingival fibroblasts over keratinocytes growth

In a typical transgingival wound healing environment, both hGF and hGK compete for implant surface colonization. Therefore, we used a 1:1 mix of hGF and hGK to test whether the different surface roughness of the titanium discs resembling enamel (M) and cementum (MA) might selectively promote the growth of a specific cell type. After 7 days, the cultures were stained for the epithelial and mesenchymal markers Laminin $\alpha 3$ (LAM $\alpha 3$) and Fibronectin (FN) (Figure S1), respectively. While the MA surface selectively impaired the growth of hGK, resulting in discs almost completely overgrown with hGF, presence of both cell types emerged on the M surface (Figure 2). These results were intriguing as hGK possess a significantly faster growth rate than hGF on tissue culture plastic (data not shown) and suggested that when both phenotypes are present, titanium implant surfaces emulating cementum (MA) markedly favored the growth of hGF over hGK.

3.3 | Titanium model substrates emulating the roughness of cementum exert cell selectivity for gingival fibroblasts by suppressing epithelial cells' proliferation

To confirm and to better understand this cell type-specific growth impairment on the MA surface, we repeated the experiments using

pure cultures of hGF and hGK. Nuclei counterstain of hGF and hGK corroborated our previous observations. While the proliferation of hGF was not affected by surface roughness as assessed by identical cell numbers on both surfaces after 7 days (Figure 3A), the growth of hGK was significantly impeded on MA compared to M surfaces (Figure 3B).

As our hGK are mixed cultures consisting of both keratinizing (e.g., positive for *Keratin 10* (K10)) and non-keratinizing (e.g., positive for *K4*) epithelial cells (Figure S2), we also included OKF6/TERT-2 in our analysis as a representative line of non-keratinizing epithelial cells, which are more similar to the sulcular epithelium, at least regarding their differentiation pattern. Nevertheless, OKF6/TERT-2 also displayed a significant growth impairment on the MA surface alike the hGK (Figure 3C).

To strengthen this observation, we further measured the gene levels of the proliferation marker *Ki67* in hGF, hGK, and OKF6/TERT-2. While *Ki67* transcript levels in hGF were comparable on M and MA surfaces, there was a clear reduction of *Ki67* in OKF6/TERT-2 as well as a trend towards lower *Ki67* in hGK when the keratinocytes were cultured on MA compared to M surfaces (Figure 3D).

To test the cytocompatibility of the novel titanium discs, we next analyzed the colony morphology of hGK and OKF6/TERT-2 keratinocytes 24 h and 7 days after seeding by staining for the actin cytoskeleton (Figure 3E,F). Typical cobblestone-like colonies were formed by hGK and OKF6/TERT-2 on both surfaces, and neither cell morphological alterations nor loss of nuclear integrity were



FIGURE 2 Competing colonization of enamel-like (M) and cementum-like (MA) surfaces by hGF and hGK. (A) Fluorescence images of 1:1 ratio co-cultured hGF and hGK on M and MA discs 7 days after seeding, stained for epithelial-specific marker Laminin $\alpha 3$ (LAM $\alpha 3$, red) and fibroblast-specific fibronectin (FN, green). Blue: cell nuclei. Scale bar: 50 μm . Close-up (right images): 20 μm .

observed after 7 days. These findings suggested that both the M and the MA surfaces allowed a normal adhesion and morphology of keratinocytes, without any signs of material-mediated cytotoxicity. Metabolic assays further confirmed that keratinocyte proliferation, but not viability, was affected on the MA surface (Figure S3).

Taken together, these data indicate that titanium model substrates with a roughness resembling cementum (MA) as opposed to enamel (M) exert cell-selective capabilities by a surface-mediated suppression of keratinocyte proliferation.

3.4 | Enamel (M) like surfaces sustain normal keratinocytes behavior. However, enhanced hydrophilicity does not provide additional benefits

As improved hydrophilicity of titanium implant surfaces has been shown to positively affect cell behavior (i.e., osteoblast adhesion and differentiation),²⁰ we were interested to analyze these processes in hGK and OKF6/TERT-2 when plated on either

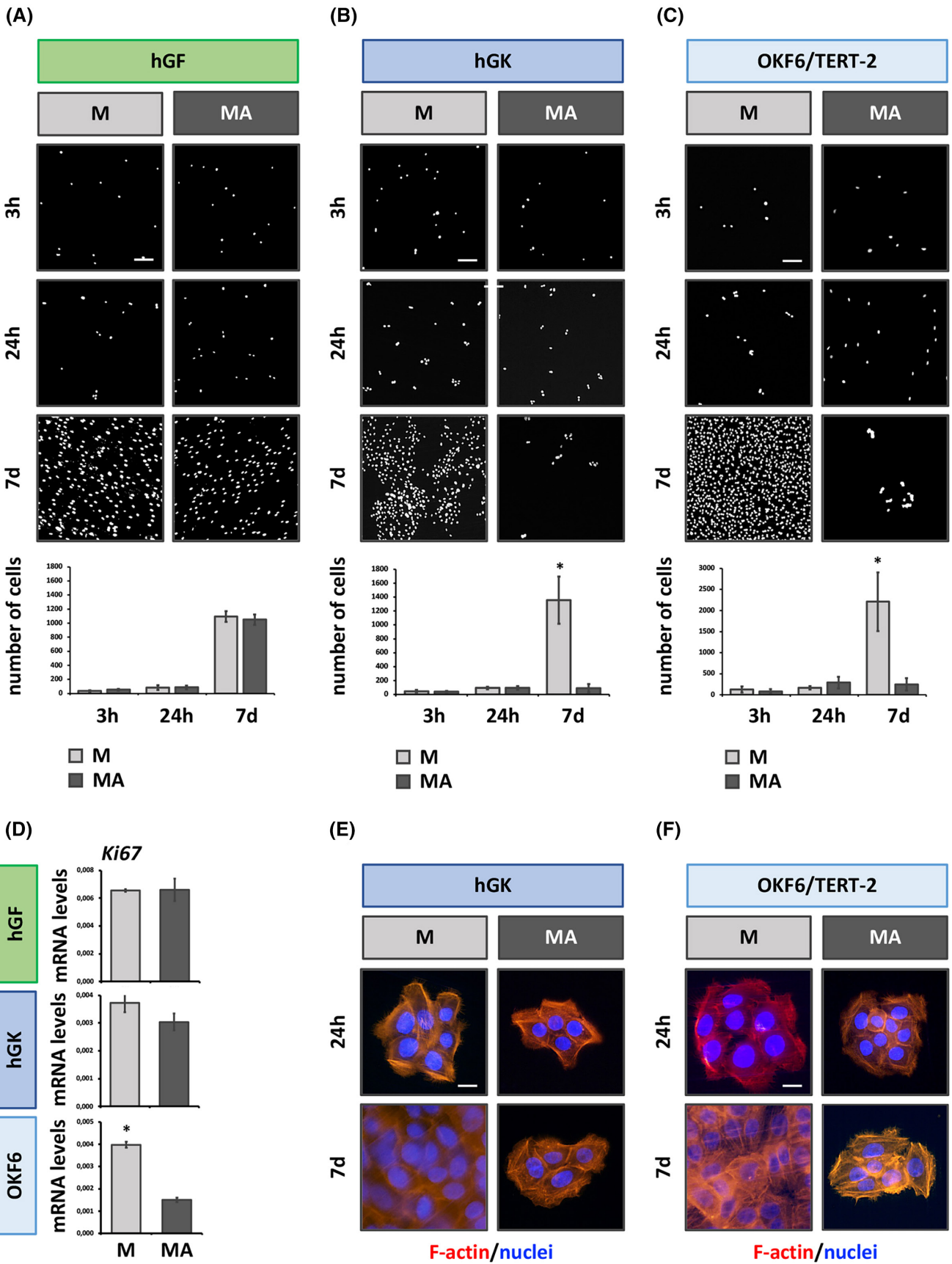
hydrophobic (M) or hydrophilic (hM) surfaces. As evidenced in Figure 4A, hydrophilicity did not influence keratinocyte adhesion and proliferation. Similar keratinocyte and colony morphologies as well as comparable cell numbers and *Ki67* transcript levels were observed 7 days post-seeding on M or hM surfaces. Identical growth was considered ideal for comparing whether the keratinocytes can still undergo their normal normally differentiation program on the M and hM surfaces. Therefore, we comparatively investigated cell density-dependent differentiation of hGK and OKF6/TERT-2 when cultured on M or hM surfaces. We specifically focused on the induction of differentiation markers distinct for non-keratinized (*K4*, *K13* and *K19*) and keratinized (*K1*, *K10* and Loricrin (*LOR*)) epithelia as well as of the more general late differentiation markers, Transglutaminase 1 (*TGM1*) and Involucrin (*IVL*). As shown in Figure 4B and in Figure S4, keratinocyte cultures could differentiate on both surfaces. However, the induction of *K1*, *K10*, and *LOR* was less pronounced in hGK on hM compared to M surfaces. In contrast, markers specific for non-keratinizing epithelia (e.g., *K4* and *K19*), except for *K13* in hGK, were similarly induced on the M and hM surfaces in both cultures. Some of these findings were further confirmed on protein level by IF. Specifically, the fluorescence images of hGK and OKF6/TERT-2 cells indicated that 7-day cultivation on both M and hM surfaces led to confluent cell layers displaying zones of stratification, although these areas seemed to be less pronounced on hM when compared to M surfaces (Figure 4C, F-Actin, white dashed lines). Similarly, *K10*-, *K13*-, *TGM1*-, and *IVL*-positive keratinocytes were generally more abundant on M compared to hM surfaces (Figure 4C and Figure S4).

Collectively, this set of data suggests that keratinocytes could attach, proliferate, and differentiate on enamel like M titanium surfaces independent of their hydrophilicity.

3.5 | Enhanced hydrophilicity of cementum (MA) like surfaces improves fibroblasts adhesion and promotes the creation of a pro-regenerative environment by modulating ECM components synthesis

According to our previous results, the use of a MA surface inhibits the gingival epithelial cell growth. Consequently, the MA surface is warranted to promote fibroblast growth.

FIGURE 3 Adhesion and proliferation of human fibroblasts and keratinocytes to M and MA titanium discs. (A–C) Fluorescence images of DAPI-labelled hGF, hGK and OKF6/TERT-2 cells on M and MA surfaces 3h, 24h, and 7 days after seeding. Histogram on the bottom reports averaged cell counts of five different regions of interest (ROIs) per substrate. Note that MA surface markedly impede the growth of human keratinocytes (i.e., hGK and OKF6/TERT-2) compared to M. h, Hours; d, Days. Scale bar: 100 μm . * $P < 0.05$. (D) Histograms showing *Ki67* transcript levels in hGF, hGK and OKF6/TERT-2 cultured on M or MA surfaces for 7 days. Note that while for hGF, *Ki67* expression is comparable on both the surfaces, *Ki67* expression on M surface is higher than MA for hGK and OKF6/TERT-2. * $p < .05$. (E, F) Fluorescence images of hGK and OKF6/TERT-2 cells on M and MA surface 24h and 7 days after seeding. Note that the underlying titanium surface did not alter cell morphology, viability, or nuclear integrity of the keratinocytes. Red: F-Actin (cytoskeleton). Blue: Cell nuclei. h, Hours; d, Days. Scale bar: 50 μm .



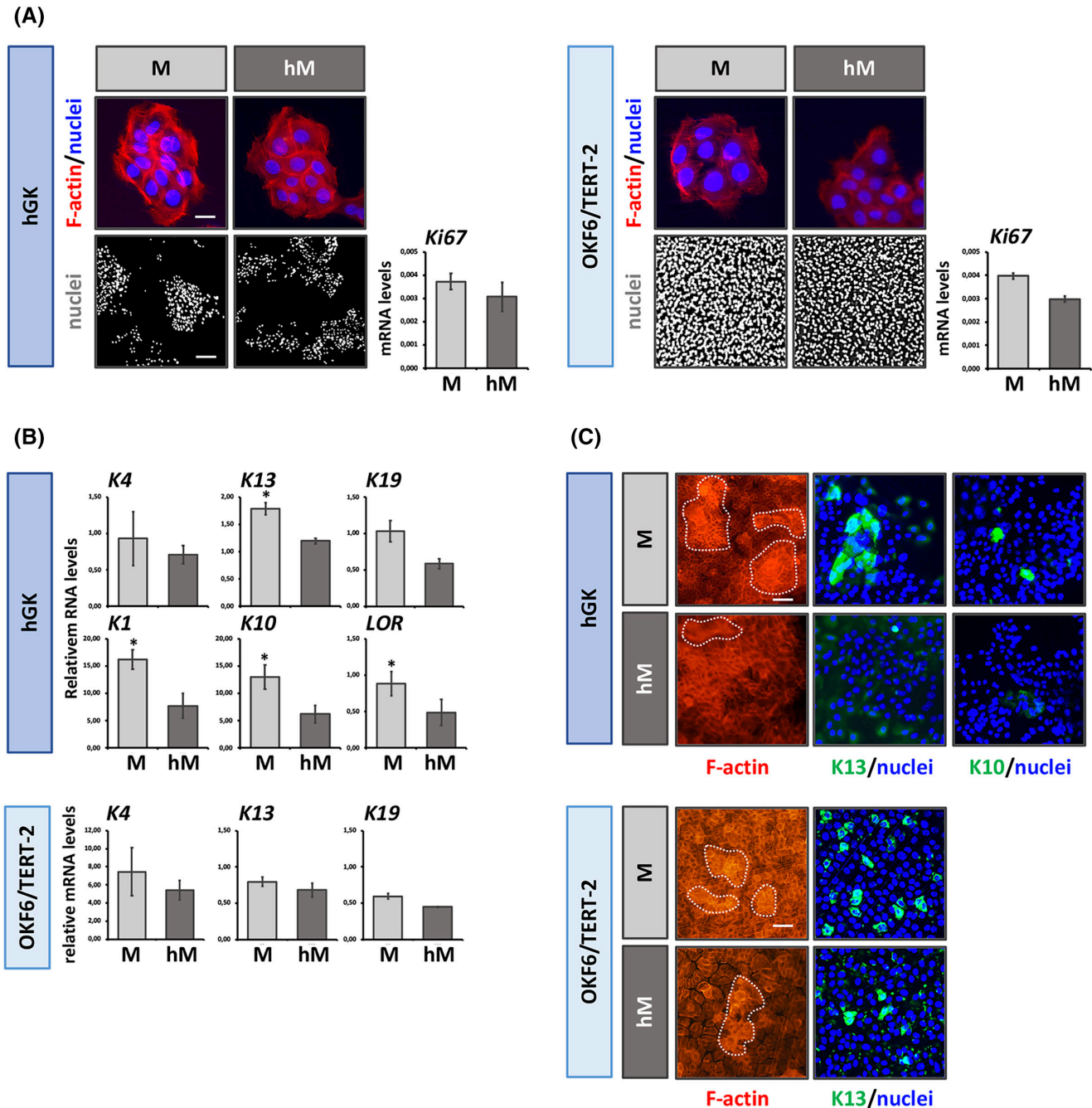


FIGURE 4 Influence of hydrophilicity of enamel-emulating M (i.e., M vs hM) surfaces towards adhesion, proliferation, and differentiation of hGK and OKF6/TERT-2 cells. (A) Fluorescence images of hGK and OKF6/TERT-2 cells on M and hM surfaces 24 h after seeding, stained for cytoskeleton (F-Actin, red) and nuclei (blue). Scale bar: 10 µm; As well as fluorescence images of DAPI-labelled hGK and OKF6/TERT-2 cells on M and hM discs 7 days after seeding. Scale bar: 100 µm. Histograms to the right report gene expression of *Ki67* in hGK and OKF6/TERT-2 cells on M and hM surfaces 7 days after seeding. Note that hydrophilicity do not impair nor promote keratinocytes adhesion and proliferation. (B) Differentiation marker expression profiles of hGK and OKF6/TERT-2 cells grown to confluency for 7 days on M and hM surface. Values have been normalized to the expression of the same genes analyzed in subconfluent cultures. K: Keratin. * $p < .05$. (C) Fluorescence images of hGK and OKF6/TERT-2 cells grown to confluency on M and hM substrates for 7 days and stained for cytoskeleton (F-Actin, red), K13 and K10 (both green). White dashed lines indicate zones of stratification. Blue: Cell nuclei. K, Keratin. Scale bar: 100 µm.

Therefore, we were interested in better elucidating the response of hGF upon encountering the MA surface resembling the natural roughness of cementum. In addition, we were also keen to learn more about the effects of hydrophilicity on the behavior of

hGF. Firstly, we investigated whether enhanced hydrophilicity could alter proliferation and adhesion of hGF on MA surfaces (Figure 5A). On both the surfaces cells appeared to be healthy displaying a canonical fibroblast morphology with an elongated spindle-like shape.

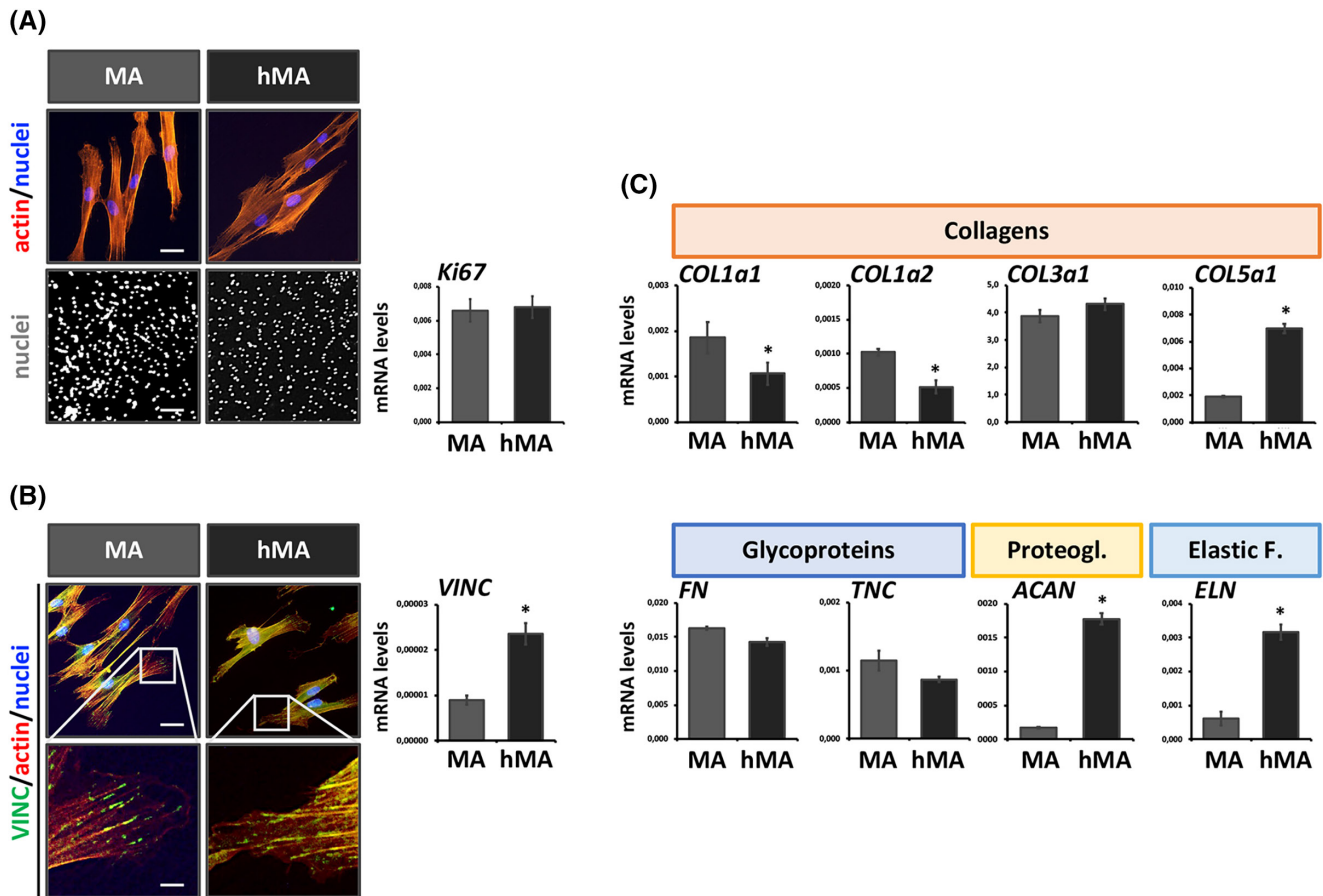


FIGURE 5 Influence of hydrophilicity of cementum-emulating MA (i.e., MA vs hMA) surfaces towards adhesion, proliferation, and gene expression of hGF. (A) Fluorescence images of hGF on MA and hMA surfaces 24 h after seeding, stained cytoskeleton (F-Actin, red) and nuclei (blue). Scale bar: 10µm. As well as fluorescence images of DAPI-labelled hGF on MA and hMA discs 7 days after seeding are also shown. Scale bar: 100µm. Histograms to the right report gene expression of *Ki67* in hGF on MA and hMA surfaces 7 days after seeding. (B) Fluorescence images of hGF on MA and hMA surfaces 24 h after seeding, stained for vinculin (VINC, green), cytoskeleton (F-Actin, red) and nuclei (blue). Scale bar: 10µm. Close-up (bottom images): 2µm. Histograms to the right report gene expression of *VINC* in hGF on MA and hMA surfaces 7 days after seeding. * $p < .05$. (C) Histograms reporting gene expression of a selected panel of extracellular matrix (ECM) components, which are representative of the main four ECM components, on MA and hMA titanium substrates 7 days after seeding: (i) collagens (orange box): Collagen 1 (*COL1a1* and *COL1a2*), 3 (*COL3a1*) and 5 (*COL5a1*); (ii) glycoproteins (blue box): Fibronectin (*FN*) and Tenascin C (*TNC*); (iii) proteoglycans (yellow box): Aggrecan (*ACAN*); and (iv) elastic fibers (light blue): Elastin (*ELN*). * $p < .05$.

Hydrophilicity did not appear to influence the proliferation of hGF as the number of nuclei after 7 days was identical on the two surfaces as were *Ki67* transcription levels. However, increased expression of Vinculin (*VINC*) was detected by qPCR in hGF cultured on hMA compared to MA (Figure 5B). In line with this observation, IF for *VINC* let us appreciate that hGF on hMA surface formed more, longer, and homogeneously distributed focal adhesions all over the cell body as compared to highly localized ones at the cell borders when plated on MA discs. Whether this potential stronger adhesion of hGF on hMA compared to M surfaces was the consequence of an altered ECM deposited by the hGF was our final question we wished to address in this study. Indeed, hydrophilicity also influenced the composition of the microenvironment produced by hGF (Figure 5B). hGF on hMA surfaces created an ECM composed of reduced levels of Collagen I (*COL1a1* and *COL1a2*) and of increased *COL5*, while *COL3a1* levels remained similar, resulting in a microenvironment surrounding

the abutment displaying a decreased *COL1/COL3* ratio, which has been often observed in scar-less, regenerative healing processes (Figure S5).³⁰ Additionally, higher levels of Aggrecan (*ACAN*) and Elastin (*ELN*) were observed in hGF on the hMA compared to MA surfaces, while the expression of *FN* and Tenascin C (*TNC*), two glycoproteins, was not affected by increased hydrophilicity.

This last set of data let us speculate that a change from hydrophobic to hydrophilic cementum-like MA surfaces may improve tight adhesion of the hGF affecting the synthesis of ECM components.

4 | DISCUSSION

Adequate peri-implant tissue quality and attachment represents one of the unresolved whilst crucial problems in modern implant dentistry.^{8,31} Indeed, while a remarkable success of over 95% has

been achieved for osseointegration,^{32,33} much lower rates have been reached for ST.² Consequently, various approaches have been developed and proposed to improve the quality of the biological seal around abutments, including engineered, micro-/nano-patterned and biopolymer-coated titanium surfaces.^{34–36} However, all these techniques come with some caveats that have impeded their clinical application, such as a cumbersome and expensive production and inability in delivery proteins in a safe and localized manner.³⁷ Hence, there is still a considerable interest in exploring titanium surface modifications which can be translated to the clinics to improve the integration of ST.

Gingival epithelial cell downgrowth and parallel arrangement of collagen fibers assembled by gingival fibroblasts are two particularities often observed around dental abutment,⁷ which have been linked to the quality of peri-implant ST. Indeed, these circumstances lead to a deeper and less sealed pocket at the implant interface, respectively. Such scenario, if combined with poor hygiene conditions and systemic disorders (e.g., diabetes), might further compromise ST integration. Consequently, guiding and improving the colonization of titanium surfaces by competing gingival fibroblasts and keratinocytes seems worth consideration.

As surface roughness is known to differentially control cell response,¹⁴ we were keen to learn whether under physiological conditions, the roughness of tooth surface might influence periodontal ST organization. Notably, we observed a stark difference between enamel and cementum roughness, which nicely corresponded with the attachment of JE keratinocytes and PDL fibroblasts, respectively. Therefore, we developed novel titanium surfaces with comparable roughness to enamel (M) and cementum (MA) (Figure 1). Knowing that gingival keratinocytes and fibroblasts are the major cell sources participating in ST integration,³⁷ we studied the behavior of patient-matched hGK and hGF when cultured on the newly developed titanium implant surfaces. We observed that although hGK possess a higher proliferation rate than hGF (data not shown), the cementum-like (MA) surface markedly impeded the proliferation of hGK in favor of hGF, without affecting their adhesion and viability (Figures 2 and 3). As such, we could conclude that the use of a bimodal rough titanium abutment, composed by an enamel-like (M) in close proximity to a cementum-like (MA) surface, could be developed to impede apical keratinocyte proliferation. Limiting epithelial cells adhesion and proliferation on the top part of the abutment would result in the formation of a shorter pocket, contrasting excessive biofilm formation.

Similar to micro-/nano-topographic cues, hydrophilicity is another characteristic affecting cells' behavior on implantable materials.³⁸ On one hand, the introduction of hydrophilicity on the M surface did not provide additional benefits on the behavior of human keratinocytes in vitro (Figure 4). On both the surfaces, signs of stratification and differentiation were indeed present. However, a slight enhancement of epithelial cells' differentiation markers (i.e., K13, K1, K10, and LOR) was noticed on the hydrophobic (M) surface. This observation could be attributed to a closer attachment of cells to hydrophilic surfaces,³⁹ which could limit the rearrangement

of cell cytoskeleton thus contrasting differentiation.⁴⁰ Whether this behavior is favorable to attain a less mature, stratified, non-keratinized and incompletely differentiated epithelium, potentially similar to the JE cannot be stated, as the keratinocytes colonizing the implant surface are embryologically different from the one giving rise to the JE.¹¹ Furthermore, we must also acknowledge that due to a limitation of the in vitro model, keratinocytes were directly seeded on the top of implantable surfaces. As in a real clinical scenario, we will never face this situation, these data must be kept as a capacity of M and hM surfaces to support a normal keratinocyte behavior in vitro, which might not necessarily reflect a better epithelial cells' response in vivo. On the other hand, we observed a strong influence of hydrophilicity on the response of hGF when cultured on the cementum-emulating discs (Figure 5). Enhanced hydrophilicity improved the adhesion of fibroblasts, as evidenced by the detection of bigger focal adhesions and higher *Vinculin* expression on the hMA versus the MA surface. Notably, the behavior of the cells reflected that observed for MG-63 and C2C12 cells when cultured on rough titanium surface with normal or increased hydrophilicity.^{39,41} Although more in depth analysis, which could better elucidate the interaction of fibroblasts with the underlying surface (i.e., SEM-FIB), would be warranted, we might speculate that an increased expression of *Vinculin* with homogeneous cytoplasmatic distribution is associated with a closer and intimate association between cells and titanium. This would be of course favorable to promote a tight seal of the CT on the implant abutment surface, and therefore, to contrast micro-motion and soft-tissue capsule formation that are known to initiate inflammation.⁴² Improved fibroblast adhesion on the hydrophilic surface was further associated with a different ECM composition. Notably, we observed a decreased ratio between *COL1a1/2* and *COL3a1* expression on the hMA surface, which let us speculate the presence of a more regenerative environment.³⁰ This observation was also strengthened by increased level of *COL5a1* on the hMA surface, whose expression has been recently associated with reduced scar size after heart injury.⁴³ Furthermore, higher transcript levels of *ACAN* and *ELN* were observed, which could suggest the deposition of a more elastic ECM on the hMA surface, and corroborating the idea of a better resistance to compression forces when a hydrophilic MA-like surface is used for CT integration.

Altogether, the herein-presented data point to combining M and MA surfaces into novel transmucosal components to optimize ST integration. However, some limitations of the present study must be reported. First of all, this is an in vitro study. In vitro models approximate more complex phenomena. In this specific case, the intricate clinical scenario was simplified by studying fibroblasts and keratinocytes behavior, while the transmucosal wound healing also involves other cell types (e.g., immune cells) and their interaction and competition with the oral microbiome. With regard to this, our findings need to be confirmed with animal studies. Another limitation of this study is the use of primary cells derived from one single donor. This choice is primarily due to the fact that for several reasons (e.g., patient age, periodontal health status) it is not

always feasible to co-isolate both epithelial cells and fibroblasts from a single tissue biopsy. However, although we acknowledge this limitation, we would like to stress the fact that using fibroblasts and keratinocytes from the same donor is definitely a strength of this study. Additionally, as we were aware of this limitation, we potentiate our data by studying the behavior of OKF6/TERT-2, an immortalized keratinocyte cell lines, which was shown to adhere, proliferate, and differentiate similarly to primary epithelial cells on the various titanium surfaces tested.

Finally, although it is not a proper limitation of this study, another aspect worth consideration regards the possibility to use a rough surface (MA) on the transmucosal component of dental implants. Indeed, as roughness is prone to bacterial contamination,⁴⁴ the use of smoother abutments has been so far advocated.⁴⁵ However, contrasting results have also been reported that a switch from the micro- to the nanoscale roughness seems to enable fibroblasts behavior while reducing bacterial attachment.^{46,47} More in vitro studies investigating the colonization of such novel implant surfaces by oral microorganisms are therefore warranted.

5 | CONCLUSIONS

In summary, the data presented within this study support the use of a bimodal roughness abutment to improve ST integration. Specifically, an apical hydrophilic cementum-emulating (hMA) surface could be combined with a coronal enamel-like (M or hM) to promote fibroblasts and epithelial cells' response, respectively. While previously postulated for cells in general,⁴⁸ the current study demonstrates for the first time that a cell-specific surface can be engineered to promote a preferential interaction with a desired cell type, at least within the context of gingival cell types. Moving forward, this phenomenon would need to be recapitulated on the tissue level to determine its clinical relevance.

AUTHOR CONTRIBUTIONS

B.B. contributed to conception, design, data acquisition and interpretation, drafted and critically revised the manuscript. B.P. contributed to conception, design, drafted and critically revised the manuscript. A.S. contributed to clinical patient samples collection and critically revised the manuscript. M.D. contributed to design, data interpretation, drafted and critically revised the manuscript. L.P. contributed to design, data acquisition and interpretation, drafted and critically revised the manuscript.

ACKNOWLEDGEMENTS

OKF6/TERT-2 cells were a kind gift of Dr. Gabriele Leyhausen, Hannover, Germany. Open access funding provided by Universitat Bern.

CONFLICT OF INTEREST STATEMENT

B.B. and B.P. are employees of Institut Straumann AG. A.S., M.D., and L.P. declare no conflict of interests.

DATA AVAILABILITY STATEMENT

The datasets generated and analyzed during the current study are available from the corresponding author on reasonable request.

REFERENCES

1. Branemark PI, Adell R, Albrektsson T, Lekholm U, Lundkvist S, Rockler B. Osseointegrated titanium fixtures in the treatment of edentulousness. *Biomaterials*. 1983;4(1):25-28. doi:[10.1016/0142-9612\(83\)90065-0](https://doi.org/10.1016/0142-9612(83)90065-0)
2. Chai WL, Brook IM, Palmquist A, van Noort R, Moharamzadeh K. The biological seal of the implant-soft tissue interface evaluated in a tissue-engineered oral mucosal model. *J R Soc Interface*. 2012;9(77):3528-3538. doi:[10.1098/rsif.2012.0507](https://doi.org/10.1098/rsif.2012.0507)
3. Kawahara H, Kawahara D, Hashimoto K, Takashima Y, Ong JL. Morphologic studies on the biologic seal of titanium dental implants. Report I. In vitro study on the epithelialization mechanism around the dental implant. *Int J Oral Maxillofac Implants*. 1998;13(4):457-464.
4. Cosyn J, Thoma DS, Hämmerle CH, De Bruyn H. Esthetic assessments in implant dentistry: objective and subjective criteria for clinicians and patients. *Periodontol 2000*. 2017;73(1):193-202. doi:[10.1111/prd.12163](https://doi.org/10.1111/prd.12163)
5. Williams D. Biomimetic surfaces: how man-made becomes man-like. *Med Device Technol*. 1995;6(1):10.
6. Ivanovski S, Lee R. Comparison of peri-implant and periodontal marginal soft tissues in health and disease. *Periodontol 2000*. 2018;76(1):116-130. doi:[10.1111/prd.12150](https://doi.org/10.1111/prd.12150)
7. Sculean A, Gruber R, Bosshardt DD. Soft tissue wound healing around teeth and dental implants. *J Clin Periodontol*. 2014;41:S6-S22. doi:[10.1111/jcpe.12206](https://doi.org/10.1111/jcpe.12206)
8. Atsuta I, Ayukawa Y, Kondo R, et al. Soft tissue sealing around dental implants based on histological interpretation. *J Prosthodont Res*. 2016;60(1):3-11. doi:[10.1016/j.jpor.2015.07.001](https://doi.org/10.1016/j.jpor.2015.07.001)
9. Berglundh T, Abrahamsson I, Welander M, Lang NP, Lindhe J. Morphogenesis of the peri-implant mucosa: an experimental study in dogs. *Clin Oral Implants Res*. 2007;18(1):1-8. doi:[10.1111/j.1600-0501.2006.01380.x](https://doi.org/10.1111/j.1600-0501.2006.01380.x)
10. Tete S, Mastrangelo F, Bianchi A, Zizzari V, Scarano A. Collagen fiber orientation around machined titanium and zirconia dental implant necks: an animal study. *Int J Oral Maxillofac Implants*. 2009;24(1):52-58.
11. Fischer NG, Aparicio C. Junctional epithelium and hemidesmosomes: tape and rivets for solving the "percutaneous device dilemma" in dental and other permanent implants. *Bioact Mater*. 2022;18:178-198. doi:[10.1016/j.bioactmat.2022.03.019](https://doi.org/10.1016/j.bioactmat.2022.03.019)
12. Guo T, Gulati K, Arora H, Han P, Fournier B, Ivanovski S. Orchestrating soft tissue integration at the transmucosal region of titanium implants. *Acta Biomater*. 2021;124:33-49. doi:[10.1016/j.actbio.2021.01.001](https://doi.org/10.1016/j.actbio.2021.01.001)
13. Ghezzi B, Lagonegro P, Attolini G, et al. Hydrogen plasma treatment confers enhanced bioactivity to silicon carbide-based nanowires promoting osteoblast adhesion. *Mater Sci Eng C Mater Biol Appl*. 2021;121:111772. doi:[10.1016/j.msec.2020.111772](https://doi.org/10.1016/j.msec.2020.111772)
14. Hou Y, Yu L, Xie W, et al. Surface roughness and substrate stiffness synergize to drive cellular mechanoresponse. *Nano Lett*. 2020;20(1):748-757. doi:[10.1021/acs.nanolett.9b04761](https://doi.org/10.1021/acs.nanolett.9b04761)
15. Kilian KA, Bugarija B, Lahn BT, Mrksich M. Geometric cues for directing the differentiation of mesenchymal stem cells. *Proc Natl Acad Sci USA*. 2010;107(11):4872-4877. doi:[10.1073/pnas.0903269107](https://doi.org/10.1073/pnas.0903269107)
16. Keselowsky BG, Wang L, Schwartz Z, Garcia AJ, Boyan BD. Integrin alpha(5) controls osteoblastic proliferation and differentiation responses to titanium substrates presenting different roughness characteristics in a roughness independent

- manner. *J Biomed Mater Res A*. 2007;80(3):700-710. doi:10.1002/jbm.a.30898
17. Wall I, Donos N, Carlqvist K, Jones F, Brett P. Modified titanium surfaces promote accelerated osteogenic differentiation of mesenchymal stromal cells in vitro. *Bone*. 2009;45(1):17-26. doi:10.1016/j.bone.2009.03.662
 18. Hotchkiss KM, Reddy GB, Hyzy SL, Schwartz Z, Boyan BD, Olivares-Navarrete R. Titanium surface characteristics, including topography and wettability, alter macrophage activation. *Acta Biomater*. 2016;31:425-434. doi:10.1016/j.actbio.2015.12.003
 19. Buser D, Brogini N, Wieland M, et al. Enhanced bone apposition to a chemically modified SLA titanium surface. *J Dent Res*. 2004;83(7):529-533. doi:10.1177/154405910408300704
 20. Gittens RA, Olivares-Navarrete R, Cheng A, et al. The roles of titanium surface micro/nanotopography and wettability on the differential response of human osteoblast lineage cells. *Acta Biomater*. 2013;9(4):6268-6277. doi:10.1016/j.actbio.2012.12.002
 21. Hotchkiss KM, Ayad NB, Hyzy SL, Boyan BD, Olivares-Navarrete R. Dental implant surface chemistry and energy alter macrophage activation in vitro. *Clin Oral Implants Res*. 2017;28(4):414-423. doi:10.1111/clr.12814
 22. Schwarz F, Sager M, Ferrari D, Herten M, Wieland M, Becker J. Bone regeneration in dehiscence-type defects at non-submerged and submerged chemically modified (SLActive) and conventional SLA titanium implants: an immunohistochemical study in dogs. *J Clin Periodontol*. 2008;35(1):64-75. doi:10.1111/j.1600-051X.2007.01159.x
 23. Edblad T, Hoffman M, Hakeberg M, Ortengren U, Milledning P, Wennerberg A. Micro-topography of dental enamel and root cementum. *Swed Dent J*. 2009;33(1):41-48.
 24. Catros S, Sandgren R, Pippenger BE, Fricain JC, Herber V, El Chaar E. A novel xenograft bone substitute supports stable bone formation in circumferential defects around dental implants in minipigs. *Int J Oral Maxillofac Implants*. 2020;35(6):1122-1131. doi:10.11607/jomi.8265
 25. Parisi L, Knapp PO, Girousi E, et al. A living cell repository of the Cranio-/orofacial region to advance research and promote personalized medicine. *Front Cell Dev Biol*. 2021;9:682944. doi:10.3389/fcell.2021.682944
 26. Degen M, Wiederkehr A, La Scala GC, Carmann C, Schnyder I, Katsaros C. Keratinocytes isolated from individual cleft lip/palate patients display variations in their differentiation potential in vitro. *Front Physiol*. 2018;9:1703. doi:10.3389/fphys.2018.01703
 27. Degen M, Natarajan E, Barron P, Widlund HR, Rheinwald JG. MAPK/ERK-dependent translation factor hyperactivation and dysregulated laminin gamma 2 expression in Oral dysplasia and squamous cell carcinoma. *Am J Pathol*. 2012;180(6):2462-2478. doi:10.1016/j.ajpath.2012.02.028
 28. Wehrle-Haller B, Koch M, Baumgartner S, Spring J, Chiquet M. Nerve-dependent and -independent tenascin expression in the developing chick limb bud. *Development*. 1991;112(2):627-637. doi:10.1242/dev.112.2.627
 29. Stavropoulos A, Sandgren R, Bellon B, Sculean A, Pippenger BE. Greater osseointegration potential with nanostructured surfaces on TiZr: accelerated vs real-time ageing. *Materials (Basel)*. 2021;14(7):1678. doi:10.3390/ma14071678
 30. Kim HY, Im HY, Chang HK, et al. Correlation between collagen type I/III ratio and scar formation in patients undergoing immediate reconstruction with the round block technique after breast-conserving surgery. *Biomedicine*. 2023;11(4):1089. doi:10.3390/biomedicine11041089
 31. Romanos GE. Tissue preservation strategies for fostering long-term soft and hard tissue stability. *Int J Periodontics Restorative Dent*. 2015;35(3):363-371. doi:10.11607/prd.2075
 32. Karoussis IK, Bragger U, Salvi GE, Burgin W, Lang NP. Effect of implant design on survival and success rates of titanium oral implants: a 10-year prospective cohort study of the ITI (R) dental implant system. *Clin Oral Implants Res*. 2004;15(1):8-17. doi:10.1111/j.1600-0501.2004.00983.x
 33. Rocuzzo A, Imber JC, Marruganti C, Salvi GE, Ramieri G, Rocuzzo M. Clinical outcomes of dental implants in patients with and without history of periodontitis: a 20-year prospective study. *J Clin Periodontol*. 2022;49(12):1346-1356. doi:10.1111/jcpe.13716
 34. Lee SW, Kim SY, Lee MH, Lee KW, Leesungbok R, Oh N. Influence of etched microgrooves of uniform dimension on in vitro responses of human gingival fibroblasts. *Clin Oral Implants Res*. 2009;20(5):458-466. doi:10.1111/j.1600-0501.2008.01671.x
 35. Marín-Pareja N, Salvagni E, Guillem-Martí J, Aparicio C, Ginebra MP. Collagen-functionalised titanium surfaces for biological sealing of dental implants: effect of immobilisation process on fibroblasts response. *Colloids Surf B Biointerfaces*. 2014;122:601-610. doi:10.1016/j.colsurfb.2014.07.038
 36. Werner S, Huck O, Frisch B, et al. The effect of microstructured surfaces and laminin-derived peptide coatings on soft tissue interactions with titanium dental implants. *Biomaterials*. 2009;30(12):2291-2301. doi:10.1016/j.biomaterials.2009.01.004
 37. Gulati K, Moon HJ, Kumar PTS, Han P, Ivanovski S. Anodized anisotropic titanium surfaces for enhanced guidance of gingival fibroblasts. *Mater Sci Eng C Mater Biol Appl*. 2020;112:110860. doi:10.1016/j.msec.2020.110860
 38. Gittens RA, Scheideler L, Rupp F, et al. A review on the wettability of dental implant surfaces II: biological and clinical aspects. *Acta Biomater*. 2014;10(7):2907-2918. doi:10.1016/j.actbio.2014.03.032
 39. Parisi L, Toffoli A, Ghezzi B, Lagonegro P, Trevisi G, Macaluso GM. Preparation of hybrid samples for scanning electron microscopy (SEM) coupled to focused ion beam (FIB) analysis: a new way to study cell adhesion to titanium implant surfaces. *PLoS One*. 2022;17(8):e0272486. doi:10.1371/journal.pone.0272486
 40. Ambriz X, de Lanerolle P, Ambrosio JR. The mechanobiology of the Actin cytoskeleton in stem cells during differentiation and interaction with biomaterials. *Stem Cells Int*. 2018;2018:2891957. doi:10.1155/2018/2891957
 41. Parisi L, Ghezzi B, Bianchi MG, et al. Titanium dental implants hydrophilicity promotes preferential serum fibronectin over albumin competitive adsorption modulating early cell response. *Mater Sci Eng C Mater Biol Appl*. 2020;117:111307. doi:10.1016/j.msec.2020.111307
 42. Eisenbarth E, Meyle J, Nachtigall W, Breme J. Influence of the surface structure of titanium materials on the adhesion of fibroblasts. *Biomaterials*. 1996;17(14):1399-1403. doi:10.1016/0142-9612(96)87281-4
 43. Yokota T, McCourt J, Ma FY, et al. Type V collagen in scar tissue regulates the size of scar after heart injury. *Cell*. 2020;182(3):545. doi:10.1016/j.cell.2020.06.030
 44. Rocuzzo A, Stähli A, Monje A, Sculean A, Salvi GE. Peri-implantitis: a clinical update on prevalence and surgical treatment outcomes. *J Clin Med*. 2021;10(5):1107. doi:10.3390/jcm10051107
 45. Morton D, Martin WC, Ruskin JD. Single-stage Straumann dental implants in the aesthetic zone: considerations and treatment procedures. *J Oral Maxillofac Surg*. 2004;62(9 Suppl 2):57-66. doi:10.1016/j.joms.2004.06.043
 46. Kearns VR, Williams RL, Mirvakily F, Doherty PJ, Martin N. Guided gingival fibroblast attachment to titanium surfaces: an in vitro study. *J Clin Periodontol*. 2013;40(1):99-108. doi:10.1111/jcpe.12025
 47. Zhu Y, Cao H, Qiao S, et al. Hierarchical micro/nanostructured titanium with balanced actions to bacterial and mammalian cells

- for dental implants. *Int J Nanomedicine*. 2015;10:6659-6674. doi:[10.2147/ijn.S92110](https://doi.org/10.2147/ijn.S92110)
48. Zhang H, Zheng X, Ahmed W, et al. Design and applications of cell-selective surfaces and interfaces. *Biomacromolecules*. 2018;19(6):1746-1763. doi:[10.1021/acs.biomac.8b00264](https://doi.org/10.1021/acs.biomac.8b00264)

SUPPORTING INFORMATION

Additional supporting information can be found online in the Supporting Information section at the end of this article.

How to cite this article: Bellon B, Pippenger B, Stähli A, Degen M, Parisi L. Cementum and enamel surface mimicry influences soft tissue cell behavior. *J Periodont Res*. 2024;00:1-13. doi:[10.1111/jre.13295](https://doi.org/10.1111/jre.13295)